ELSEVIER

Journal of Photochemistry and Photobiology A: Chemistry 105 (1997) 225–233

Journal of PHOTOCHEMISTRY AND PHOTOBIOLOGY A:CHEMISTRY

Intramolecular transfer of excitation energy in short linear peptides carrying naphthalene and protoporphyrin molecules. A molecular model of electron transfer/energy transfer transition

B. Pispisa [a,*], M. Venanzi [a], A. Palleschi [b], G. Zanotti [c]

[a] *Dipartimento di Scienze e Tecnologie Chimiche, Universita' di Roma "Tor Vergata", Via Ricerca Scientifica, 00133 Roma, Italy*

[b] *Dipartimento di Chimica, Università di Roma "La Sapienza", Piazzale A. Moro, 00185 Roma, Italy*

[c] *Centro di Chimica del Farmaco del CNR, c/o Dipartimento di Chimica Farmaceutica, Università di Roma "La Sapienza", Piazzale A. Moro, 00185 Roma, Italy*

Received 11 September 1996; accepted 12 September 1996

Abstract

Sequential oligopeptides carrying naphthalene and protoporphyrin IX as fluorophores, covalently bound to ϵ-amino groups of lysine residues, were investigated in methanol and water/methanol 75/25 (v/v) solutions by steady-state fluorescence, transient absorption spectra and time resolved emission measurements. Quenching of excited naphthalene chiefly takes place by transfer of excitation energy, $^1N^* \rightarrow P$, and proceeds on a time scale of 3–8 ns (25 °C), depending on the helical periodicity of the backbone chain. According to earlier IR and CD spectral results, the oligopeptides investigated attain an α-helix conformation, which is responsible for the periodic variation of the interprobe distances. A slower ($\approx$45 ns) and minor fluorescence decay was also measured, which is ascribed to exciplex emission. This finding differs from that earlier obtained with the same chromophores bound to α-helical poly(L-lysine) in water, where quenching of naphthalene was mainly due to electron transfer from ground-state porphyrin, $P \rightarrow {}^1N^*$. Molecular mechanics calculations show a different topology of N and P molecules bound to the α-helix in the two systems, which is thought to be primarily responsible for the observed transition between photoinduced electron transfer and energy transfer. © 1997 Elsevier Science S.A.

Keywords: α-Helical short linear peptides; Electron transfer/energy transfer transition; Molecular mechanics calculations; Naphthalene chromophores; Protoporphyrin IX chromophore; Ps and ns transient spectra

1. Introduction

Model systems formed by a variety of molecules carrying covalently bound porphyrins have been used for studying naturally-occurring, light-initiated reactions [1–3]. To mimic a natural environment, macromolecular materials [4], especially synthetic polypeptides [5,6], were often employed as carriers, though fluorescent probes have also proved to be a valuable tool for obtaining important details on conformational features and dynamics of the polymeric matrix in solution [7–9].

To address the problem of the dynamics of biomimetic systems in aqueous solution, we started investigating the photophysical behavior of protoporphyrin IX and 1-naphthylacetic acid covalently bound to ϵ-amino groups of poly(L-lysine) [6,10]. On going from pH 7 to 11, i.e. from the disordered to the ordered polymeric matrix, quenching of excited naphthyl chromophores was found to chiefly occur by two competitive processes. One was interconversion to the triplet state, taking place when the sample was randomly coiled, and the other intramolecular electron transfer from ground-state porphyrin, when the polypeptide was in α-helical conformation [6]. Kinetic results coupled with conformational statistics data showed that the rate constant of the photoinduced electron transfer at $\langle R \rangle \approx 12$ Å, corresponding to the average interchromophoric distance for which the transfer has the highest probability of occurring, was $4.0 \times 10^7\ s^{-1}$, in very good agreement with that experimentally determined, i.e. $3.1 \times 10^7\ s^{-1}$ (25 °C) [10]b. They also suggested that the coil $\rightleftharpoons$ α-helix transition takes place on a time scale around 20 ns, while the librational motion of the probe linkages occurs on a time scale of a few nanoseconds [10].

More recently, we have studied the photophysical behavior in methanol and water/methanol 75/25 (v/v) solution of sequential oligopeptides carrying the same chromophores,

* Corresponding author.

PII S1010-6030(96)04494-2

i.e. protoporphyrin IX (P) and naphthalene (N), covalently bound to the ϵ-amino group of L-lysine (Lys) residues. The peptide building block was the Leu–Leu–Lys triad, where Leu denotes L-leucine, and the oligopeptides were obtained by combining two such triads through a spacer consisting of $n=0$–4 alanine (Ala) residues. In all cases the backbone chain was found to attain an ordered conformation [11–13], owing to the good α-helix propensity of Leu and Ala residues [14], though, contrary to expectation, quenching of naphthalene fluorescence was found this time to occur by intramolecular transfer of excitation energy, $^1N^* \rightarrow P$ [12,13]. We were then able to satisfactorily reproduce the transfer efficiency [13], using the long-range dipole–dipole interaction model [15], according to Eq. (1),

$$E_t = R_0^6/[R_0^6 + (2R^6/3k^2)] \quad (1)$$

where R is the interchromophoric distance, R_0 the critical distance at which transfer and spontaneous decay of excited donor are equally probable, and k^2 a dimensionless geometric factor determined by the orientation in space of the transition dipole moments of the donor, N, and acceptor, P, as given by Eq. (2) [16,17]. The donor and acceptor molecules were, in fact, found to rotate slowly on the time scale of the transfer process, being thus unable to randomize their orientation during the donor lifetime. A particular relative orientation between N and P is then described by two angles only, γ and θ, where $0 \leq \gamma$, $\theta \leq \pi$, i.e. [13,16]

$$k^2 = \cos^2\theta(3\cos^2\gamma + 1) \quad (2)$$

In this paper we present transient absorption spectra in methanol and water/methanol 75/25 (v/v) on both nanosecond and picosecond time scales of P(Ala)$_n$N oligopeptides, as those illustrated in Scheme 1, together with new steady-state fluorescence results on the same peptides and on (Ala)$_n$N and (Ala)$_n$P blanks. By using the most relevant fluorescence data previously reported [12,13] and the new photophysical results we were able to gain a better insight into the excited-state properties of the compounds examined, and to account for the topological conditions for the electron transfer/energy transfer transition occurring in the ordered polypeptides/oligopeptides investigated.

2. Experimental

2.1. Materials

The synthesis of the oligopeptides was performed by the conventional mixed anhydride method, as extensively described elsewhere [11,12]. Amino acid precursors were purchased from NOVA Biochem or Fluka, and naphthylacetic acid and protoporphyrin IX from Aldrich. Analytical-grade reagents and solvents were always used.

Identity and purity of all peptides were checked by amino acid, ^{1}H NMR, high resolution mass spectrometry (FAB), and thin-layer chromatography analyses, this latter making use of silica gel Merck plates. In Scheme 1, Boc and OtBu stand for *tert*-butyloxycarbonyl and *tert*-butyl ester, respectively.

Boc- Leu-Leu-Lys-(Ala)$_n$-Leu-Leu-Lys-*OtBu*

P N

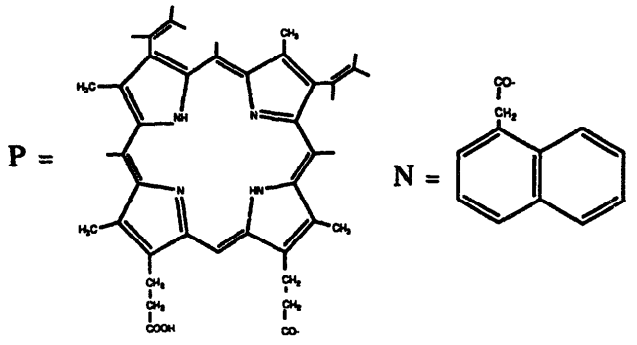

Scheme 1.

Spectroscopically pure methanol (Merck) and doubly distilled water were used as solvents for spectroscopic measurements.

2.2. Methods

Transient absorptions in the nanosecond time scale were performed by a flash-photolysis set-up, the pulsed excitation (308 nm) being achieved by a Xe/HCl excimer laser (Lamda Physik EMG 50E). The pulse width was about 15 ns, the laser energy less than 10 mJ pulse^{-1}, and the delay time < 1 ns. The light (150 W Xe lamp) was examined through a Baird–Tatlock monochromator, a Hamamatsu R928 photomultiplier and then captured by a Tektronix DSA602 transient digitizer.

Transient absorption measurements in the picosecond time scale were carried out at the European Laboratory of Non-Linear Spectroscopy (Florence). Subpicosecond pulses at 580 nm were obtained by a dye laser (Rhodamine 6G) pumped by a fiber compressed ML Nd-YAG laser. A 10% fraction was focussed in a water cell, producing white light (350–820 nm), while the rest was collimated in a 0.6 BBO crystal to produce the 290 nm pulses used to excite the sample. One part of the white light was sent to a computer-controlled optical delay time line and then focussed again to the sample (1 cm cuvette, magnetically stirred) with both the other part of the white light and the excitation beam. The transient absorptions were obtained taking the ratio of the two spectra produced by part of the white light and by the remaining of the white light in coincidence with the excitation beam. The two spectra were separately sent to the linear diode arrays of a double OMA detector, and recorded as a function of the time delay between the excitation and the probe pulses.

Steady-state fluorescence spectra were recorded in quartz cells by a SPEX Fluoromax spectrofluorometer, operating in the SPC mode ($\lambda_{ex}=280$, $\lambda_{em}=340$ nm, unless otherwise stated), while fluorescence anisotropy measurements were

carried out on the same apparatus, equipped with Glan–Thompson polarizing prisms. Nanosecond decays were measured by a homemade SPC apparatus (ORTEC electronics, optics from Applied Photophysics, nanosecond coaxial flashlamp (FWHM = 2.0 ns) from Edinburgh Instruments). Excitation in the UV region was achieved by ultrapure deuterium as filling gas (0.400 mm Hg). The decay curves were fitted by a non-linear least-squares analysis to exponential functions by an iterative deconvolution method. All solutions were bubbled for about 20 min with ultrapure nitrogen before each measurement.

Absorption spectra were recorded on a Jasco 7850 apparatus with appropriate quartz cells. Other apparatus have already been reported [11,12].

3. Results and discussion

3.1. Polarized fluorescence and transient absorption spectra

Fig. 1 illustrates the dependence of the fluorescence anisotropy coefficient, $r=(I_{\parallel}-I_{\perp})/(I_{\parallel}+2I_{\perp})$, of $P(Ala)_nN$ in methanol and water/methanol 75/25 (v/v) on the number of Ala units in the spacer, n. Since the decay times of the species investigated are very similar in both solvent media, as shown below, the linear relationship between r and n is ascribable to hindered internal Brownian motions of the probes linkages, the effect being greatly enhanced by adding water. This suggests that hydrophobic interactions between the apolar P and N groups stiffen the whole structure, the greater the longer the backbone chain; a conclusion supported by circular dichroism spectra (not shown) exhibiting extrinsic CD bands in the ^1B_b and ^1C_b absorption region of naphthalene, despite its location being far from the chiral C^{α} atom [11].

We next investigated the transient absorption spectra of both blanks and oligopeptides in the two solvent media. Typical spectra in methanol are shown in Fig. 2, where the bleaching of the Soret band at 400 nm [18], the characteristic triplet–triplet absorption of protoporphyrin at around 320 and 470 nm [18,19], and weak absorption structures at lower energies, possibly ascribable to radical anions, are observed.

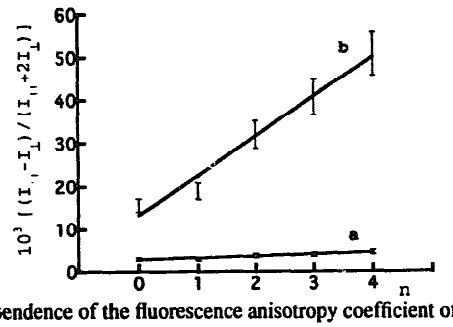

Fig. 1. Dependence of the fluorescence anisotropy coefficient of $P(Ala)_nN$ peptides on the number of Ala units in the spacer ($\lambda_{ex}=280$, $\lambda_{em}=340$ nm). Curve a, methanol; b, water/methanol 75/25 (v/v) solution.

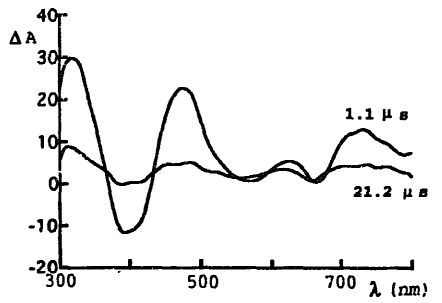

Fig. 2. Typical transient absorption spectra in methanol. They refer to $P(Ala)_3N$, after 1.1 and 21.2 μs. Note the bleaching of the Soret band at 400 nm and the triplet–triplet transitions at around 320 and 470 nm.

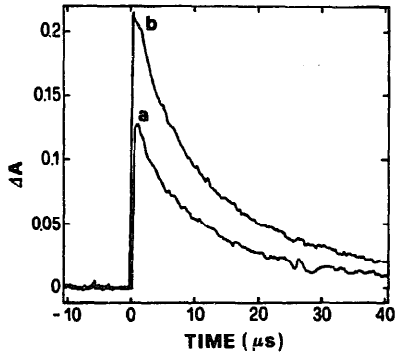

Fig. 3. Kinetics of the triplet states decay in methanol, at 25 °C. Curve a, 470 nm band; b, 320 nm band.

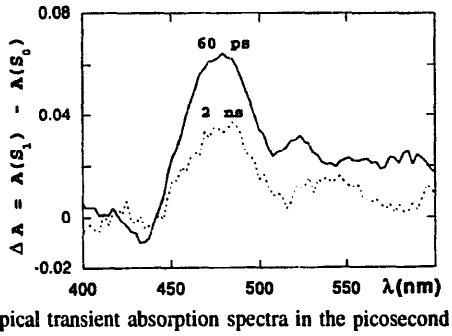

Fig. 4. Typical transient absorption spectra in the picosecond time scale. They refer to the octapeptide, $P(Ala)_2N$, in methanol, showing the band, centered at around 480 nm, of $P^*(S_n) \leftarrow P^*(S_1)$ transitions, still detected after 2 ns.

The lifetime of the triplet states is around 11–13 μs, corresponding to a decay rate constant of about 8×10^4 s^{-1} (Fig. 3), while kinetic measurements of oxygen saturation show that the second-order rate constant for bleaching the 320 and 470 nm absorptions is around 1.8×10^9 M^{-1} s^{-1} (25 °C), in good agreement with the second-order rate constants for triplet quenching by O_2 [18–20].

Transient absorption spectra in the picosecond time scale show that, under the same conditions, the quickly populated $P^*(S_1)$ state is long-lived, the broad band corresponding to $P^*(S_n) \leftarrow P^*(S_1)$ transitions, centered at around 480 nm, still being detected after 2 ns (Fig. 4).

By contrast, transient absorption spectra in water/methanol 75/25 exhibit no T–T transitions. In Fig. 5 a typical example of transient absorptions in a 60/40 (v/v) water/methanol mixture is reported, showing the bleaching of the

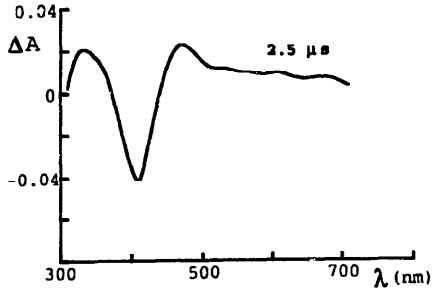

Fig. 5. Transient absorption spectrum of $P(Ala)_2N$ in water/methanol 60/40 (v/v), after 2.5 μs, showing very weak T–T transitions at 320 and 470 nm, that completely disappear by further addition of water.

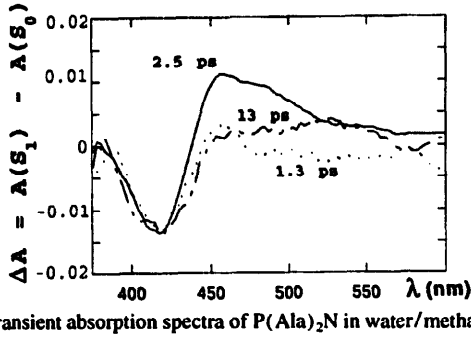

Fig. 6. Transient absorption spectra of $P(Ala)_2N$ in water/methanol 75/25 in the picosecond time scale. The fastly rising absorption at 450 nm is very likely ascribable to a transition with an intramolecular charge-transfer character (see text).

Soret band at 400 nm and very weak T–T transitions at around 320 and 470 nm, that completely disappear by further addition of water. Under the same conditions, in the picosecond time scale the bleaching of the Soret band is accompanied by a new band at 450 nm, as shown in Fig. 6. The quickly rising 450 nm absorption is most likely due to a transition with an intramolecular charge-transfer character because it disappears in less polar solvents, such as methanol or dioxane. We represent the excited complex as $(P^{\delta+} - N^{\delta-})^*_{solv}$, where δ is the degree of partial charge transfer, and the subscript solv denotes hydration effects owing to the clusters of water molecules that are likely to surround this bulky, apolar complex. Its lifetime is very short, i.e. about 10 ps, suggesting that the major pathways for the non-radiative deactivation could be vibronic interactions with these clusters of solvent, an idea fully consistent with both the efficiencies of the quenching process reported below, and the role of hydrophobic interactions in stabilizing compact structures of apolar moieties in water, even in the excited state.

3.2. Steady-state fluorescence spectra

A typical example of steady-state fluorescence spectra in methanol and water/methanol 75/25 (v/v) is illustrated in Fig. 7. Besides a weak exciplex emission ($\approx$425 nm; inset in the figure), which is further depressed as the polarity of the solvent increases, a substantial quenching of N singlet emission by the bound protoporphyrin molecule can be noted.

The fluorescence quantum yield of the oligopeptides in both solvent media (Φ_{PN}) and the efficiency of the quenching

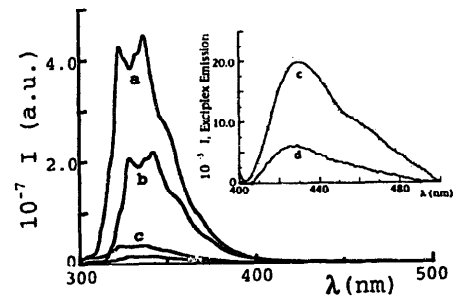

Fig. 7. Steady-state fluorescence spectra of $(Ala)_2N$ (curves a and b) and $P(Ala)_2N$ (c and d), in methanol (a and c) and water/methanol 75/25 (b and d); $\lambda_{ex} = 280$ nm. Besides the weak exciplex emission (insert), a substantial quenching of N singlet emission by protoporphyrin can be noted.

process, E_N, as given by $[1 - (\Phi_{PN}/\Phi_N)]$, are reported in Table 1. The quantum yield of the blanks, carrying the N group only (Φ_N), is quite similar to that of free naphthalene [21], indicating that naphthyl–peptide interactions are absent or very weak.

By inspection of the Table, it appears that E_N in methanol parallels with the efficiency of the fluorescence rise in P, E_P, thus indicating that the energy lost in the deactivation of the excited naphthyl chromophore is nearly completely transferred to the porphyryl group, apart from the minor exciplex emission.

Quenching of N* in water/methanol 75/25 shows, instead, that the fluorescence quantum yield of P is negligibly small, so that E_P is unmeasurable. Since titration with H_2O of, for example, $P(Ala)_2N$ and $(Ala)_2P$ in methanol brings about the complete bleaching of the T–T band at 470 nm, while, at the same time, the quantum yields of porphyrin emission in the range of 600–720 nm ($\lambda_{ex} = 308$ nm) dramatically decrease (Table 2), it may be concluded that addition of water up to 75% (by vol) into the methanol solution turns off the usual channels of the excited states relaxation of porphyrin, i.e. interconversion to the triplet and singlet states, opening new efficient non-radiative pathways for the dissipation of the energy transferred to P, as mentioned above.

Table 1
Energy transfer efficiencies in methanol and water/methanol 75/25 (v/v), from steady-state measurements

Sample	Methanol		Water/methanol	
	E_N [a]	E_P [b]	E_N [a]	E_P [b]
$P(Ala)_0N$	0.61	0.58	0.76	
$P(Ala)_1N$	0.59	0.53	0.58	
$P(Ala)_2N$	0.82	0.78	0.84	
$P(Ala)_3N$	0.77	0.66	0.68	
$P(Ala)_4N$	0.55	0.43	0.62	

[a] $\lambda_{ex} = 280$, $\lambda_{em} = 340$ nm; $E_N = 1 - (\Phi_{PN}/\Phi_N)$. Φ_{PN} is the quantum yield of N* in $P(AA)_nN$ and Φ_N ($\approx$0.22) that in $(AA)_nN$.

[b] $\lambda_{ex} = 280$, $\lambda_{em} = 630$ nm; $E_P = [(I_{PN}/I_P) - 1] \cdot (\epsilon_P C_P/\epsilon_N C_N)$, where $I_P = \epsilon_P C_P \Phi_P$ and $I_{PN} = \epsilon_P C_P \Phi_P + \epsilon_N C_N \Phi_P E_P$ are the fluorescence intensities of porphyrin in $(AA)_nP$ and in $P(AA)_nN$, respectively, while C_P and C_N are the concentration of the acceptor and donor chromophores. In all cases, the uncertainty is better than 6%.

Table 2
Dependence of relative quantum yields of porphyrin emission on added water [a]

% H_2O (by	0	25	50	75
$P(Ala)_2N$	1	0.604	0.181	0.057
$(Ala)_2P$	1	0.702	0.401	028

[a] $\lambda_{ex}=308$ nm; sample concentration 1.4×10^{-6} M. The emission range explored was 600–720 nm; the uncertainty is within 10%.

Aggregation effects of P on the observed phenomena can be ruled out because the P emission intensity follows Beer's law by changing the concentration of one order of magnitude, even in water/methanol 50/50 (v/v).

Interestingly, further inspection of Table 1 also indicates that the quenching efficiency of $P(Ala)_nN$ in both solvent media goes through a maximum as n increases, in agreement with the helical periodicity of the C^{α} atoms of the probes linkages. In this case more Ala intervening residues do not necessarily mean a greater separation distance between the chromophores.

To summarize, the foregoing results on the emission behavior of porphyrin and the finding that no absorption in the transient spectra can be ascribed to a radical cationic moiety, i.e. $P^{\cdot+}$ [10,20,22], lead us to conclude that quenching of naphthalene by porphyrin cannot be due to a $P\rightarrow {}^1N^*$ electron transfer process, as previously observed with α-helical poly(L-lysine) carrying the same chromophores [6,10],

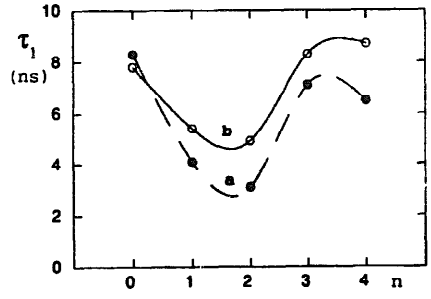

Fig. 8. Dependence of the decay time of the singlet naphthyl state by energy transfer on the number of alanyl units in the spacer. Curve a, methanol; , b, water/methanol 75/25 solution. The trend of τ_1 reflects the α-helix periodicity.

but rather to electronic energy transfer between the energetically excited donor and the ground-state acceptor. Furthermore, addition of water into the methanol solutions of the peptides investigated does not significantly alter the dynamic relaxation behavior of the probes, but affects the dissipation mechanism of the energy transferred to P.

3.3. Time-resolved emission data

The results of fluorescence time decays of excited naphthalene in methanol and water/methanol 75/25 (v/v) were found to be very similar, within experimental errors [12,13]. In addition, in all cases no significant change was observed on varying samples concentration within one order of magnitude (2×10^{-6} to 2×10^{-5} M), so that interchain effects can be ruled out.

The curves were well fitted by a two-component exponential decay, Eq. (3), while the time decay of the blanks, τ_0, was always found to be strictly monoexponential [12,13].

$$I(t)=\alpha_1\exp(-t/\tau_1)+\alpha_2\exp(-t/\tau_2) \quad (3)$$

The shorter decay time, τ_1, ranges from 3 to 8 ns, as shown in Fig. 8, and can be assigned to the energy transfer process. The longer decay time, τ_2, measures the exciplex decay, being insensitive to interchromophoric distance. This assignment is supported by the fact that decay measurements at $\lambda_{em}=470$ nm, where the N* emission is definitely minor, show a similar dominant long lifetime component, which is affected, unfortunately, by a rather large uncertainty, owing to the very low fluorescence emission within this wavelengths region.

As already pointed out, the trend of τ_1 as a function of the alanyl units in the spacer (Fig. 8), similar to that of transfer efficiency (Eq. (4)) shown later, reflects the helix periodicity of the backbone chains. Furthermore, from the data of Table 3, where decay times and pre-exponents are listed, it appears that the pre-exponent of the long component, α_2, is much larger for the hepta- and decapeptides than for the other samples. Since this quantity measures the relative population of the species undergoing exciplex decay, this finding is very like due to the fact that the probes in $P(Ala)_1N$ and $P(Ala)_4N$ are on the same side of the α-helix, one or two turns apart,

Table 3
Fluorescence lifetimes of N* in methanol and water/methanol 75/25 (v/v) at 25 °C [a]

Sample	Methanol					Water/methanol				
	τ_1 (ns)	α_1	τ_2 (ns)	α_2	χ^2	τ_1 (ns)	α_1	τ_2 (ns)	α_2	χ^2
$P(Ala)_0N$	8.3	0.85	45.5	0.15	1.40	7.8	0.88	45.5	0.12	1.40
$P(Ala)_1N$	4.1	0.62	46.0	0.38	1.15	5.4	0.56	45.0	0.44	1.69
$P(Ala)_2N$	3.1	0.93	45.6	0.07	1.05	4.9	0.95	45.0	0.05	1.41
$P(Ala)_3N$	7.1	0.82	44.2	0.18	1.18	8.3	0.83	45.0	0.17	1.41
$P(Ala)_4N$	6.5	0.59	46.0	0.41	1.53	8.7	0.71	45.0	0.29	1.80

[a] $\lambda_{ex}=280$, $\lambda_{em}=340$ nm; the time decay of N* in the $(Ala)_nN$ (blanks) is $\tau_0=52.5\pm1.5$ ns in methanol and 36.2 ± 1.6 ns in water/methanol 75/25. In all cases the lifetimes uncertainty is better than 5%, while that of the pre-exponents is around 20%.

respectively, favoring a proper arrangement for exciplex formation [5].

$$E_t = 1 - (\tau_t/\tau_0) \quad (4)$$

Taken together, all these features allow us to formulate the decay pathways illustrated in Schemes 2 and 3 for the peptides in methanol and water/methanol 75/25 solutions, respectively. Accordingly, the excited singlet naphthalene in methanol primarily transfers its electronic energy to the Soret $P^*(S_2)$ state, which, in turn, very quickly populates porphyrin singlet and triplet states. Instead, the same $P^*(S_2)$ species in water/methanol 75/25 quickly decays into a solvated, intramolecular charge-transfer state, which undergoes an efficient, non-radiative deactivation process.

Finally, where an average transfer efficiency, $\langle E_t \rangle$, comprising the parameter k^2 (Eq. (2)) that takes into account the angular relationship between the chromophores, is evaluated according to the conformational statistics analysis already

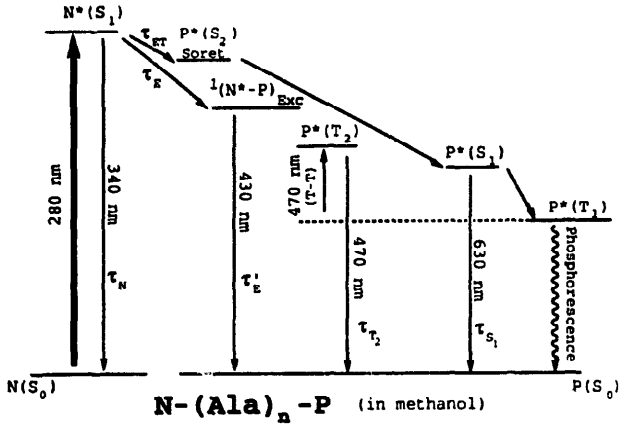

Scheme 2.

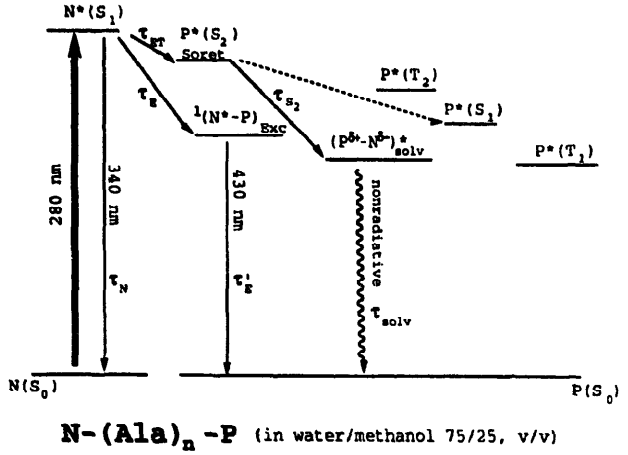

Scheme 3.

Table 4
Comparison between calculated [a] and experimental [b] energy transfer efficiency, in methanol and water/methanol 75/25 (v/v)

Sample	Methanol		Water/methanol	
	$\langle E_t \rangle$ [a]	E_t [b]	$\langle E_t \rangle$ [a]	E_t [b]
$P(Ala)_0N$	0.881	0.84	0.831	0.79
$P(Ala)_1N$	0.933	0.92	0.893	0.85
$P(Ala)_2N$	0.928	0.94	0.840	0.86
$P(Ala)_3N$	0.885	0.86	0.760	0.77
$P(Ala)_4N$	0.891	0.88	0.772	0.76

[a] From conformational statistics analysis of the probes linkages, with the backbone chain in α-helix, and taking also into account the relative orientation of N and P chromophores by Eq. (2) [12,13].
[b] From Eq. (4), the uncertainty being within 8%.

reported [12,13], the results listed in Table 4 are obtained. This because the interprobe distances distribution cannot be ignored, owing to both the α-helix periodicity of the C^α atoms carrying the chromophores and the conformational mobility of the hydrocarbon portion of the probes linkages (Scheme 1). Calculations were based on the rotational isomeric state model for the probe linkages [26], with the backbone chain fixed in the α-helix conformation [12,13].

The main inference to be drawn from Table 4 is that the good agreement between $\langle E_t \rangle$ and E_t, as given by Eq. (4), indicates that the orientation of the chromophores is not randomized during the donor lifetime. If the "dynamic" isotropic average of the orientation factor, $\langle k^2 \rangle = 2/3$ [9,16,17], would have been used instead of Eq. (2), implying a free internal rotation of the probes, the $\langle E_t \rangle$ values would have been as high as 0.96–0.99 in all cases. In addition, the agreement improves as the length of the peptides increases because in the calculations the backbone was fixed in the α-helix geometry, and this assumption holds true the longer the backbone chain [11].

3.4. Electron vs. energy transfer in the α-helical systems investigated

We now address the issue of why there is a transition between photoinduced electron transfer and energy transfer in the quenching process of N* on going from the polypeptide in water to the oligopeptides in water/methanol 75/25. From a phenomenological point of view it reflects a transition between exponential [23–25] and inverse sixth power [12]b[15] behavior with respect to the donor–acceptor distance R.

Both polypeptide and oligopeptides are in the α-helix conformation and carry the same chromophores covalently bound to the ε-amino groups of Lys residues. In addition, the viscosity of the solvent media is nearly the same, and the presence of water in the peptides solution stabilizes the α-helix, discouraging dynamic distortions in the short helical segments [12]a[27]. The conformational rigidity of the two systems is thus expected to be comparable. Therefore, the

effect should primarily arise from different topological conditions. To check this hypothesis, we performed molecular mechanics calculations, as reported below.

Earlier data of theoretical conformational analysis on the α-helical poly(L-lysine) carrying P and N molecules had shown that the most sterically favorable arrangement of the bound chromophores is that in which they are almost frozen on the surface of the α-helix, with the equatorial plane lying parallel to the helical axis of the polymer, whatever the center-to-center separation distance [6].

We now apply Eq. (5) [28] to both α-helical systems, the total energy function comprising stretching and bending terms, besides non-bonding, electrostatic and torsional potentials similar to those previously employed by us [6,13,29].

$$U_{tot} = NB + COUL + TOR + STR + BEN \quad (5)$$

NB and COUL are the sum of all pairwise non-bonded and electrostatic interactions, respectively, where a 6-12 LJ potential function for the non-bonded interatomic interactions, and partial atomic charges for each atom in the systems investigated were used. TOR is the torsional potential function, as given by Eq. (6), where s is the number of torsional rotations around the dihedral angle χ_k.

$$TOR = \sum_{k=1}^{s} \sum_{f=1}^{3} \frac{V_{0kf}}{2} [1 + \cos(f\chi_k - \phi)] \quad (6)$$

Finally, the last two energetic terms refer to the sum over all bonds for stretching and all angles for bending modes, i.e.

$$STR = \sum_{bonds} k_s (d - d_0)^2 \quad (7)$$

$$BEN = \sum_{angles} k_b (\theta - \theta_0)^2 \quad (8)$$

where k_s and k_b are the force constants for each mode, and $(d - d_0)$ and $(\theta - \theta_0)$ the displacement from the equilibrium value of bonds and angles, respectively [28].

Computational details will be reported elsewhere, while the most relevant results can be summarized as follows. (1) The energy profile of bound porphyryl-polypeptide and bound naphthyl-polypeptide, reported in Fig. 9, clearly indicates that the energetically most favorable structures are those in which the probes rings are in close contact with the ordered backbone chain, in a parallel or almost parallel fashion with respect to the α-helical axis. (2) The closest separation distance between the center of P and N molecules and this axis is 5.80 and 5.26 Å, while the angle of the axis normal to the equatorial plane of the probes with the helical axis is about 85° and 75°, respectively. (3) The side-chains of the polymeric matrix provide a cage-like structure where both the porphyryl and naphthyl rings are almost frozen in. (4) This type of arrangement is expected to be further stabilized in aqueous solution by entropic effects, because contacts between the bound apolar N and P groups and solvent molecules are minimized. (5) Attempts to build up a stacked geometry, where naphthalene is sandwiched between the

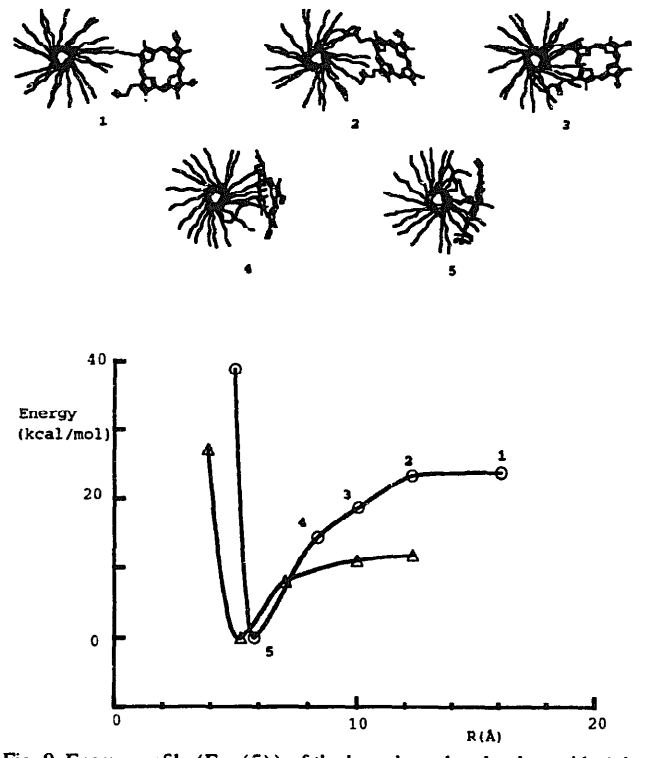

Fig. 9. Energy profile (Eq. (5)) of the bound porphyryl-polypeptide (circles) and naphthyl-polypeptide (triangles) as a function of the separation distance of the center of P and N from the helical axis. Both chromophores approach the α-helix from the fully extended conformation of the probe linkage. Each step corresponds to a local structure in the deepest energy minimum, as schematically illustrated at the top of the plot for the bound porphyrin moiety, viewed along the helical axis of the poly(L-lysine).

helix and porphyrin or vice versa in a face-to-face fashion, led to structures having energies higher than or comparable to those with an edge-to-edge arrangement (Fig. 10), provided that the center-to-center distance was shorter than 4 Å. This separation distance appears too small, however, as compared to the average interchromophoric distance for which electron transfer has the highest probability to occur, i.e. 12 Å [10]b. Indeed, a face-to-face arrangement seems also unlikely in view of the high dilution of the probes over the helix [10].

All these features are reminiscent of those already observed for hemin-like quaterpyridineiron(III) complex ions bound to helical poly(L-glutamate) [29]a, and are similar to those earlier obtained by theoretical conformational calculations [6], apart from some distortions in the α-helix. They are also fully consistent with the extrinsic ellipticity of the bound achiral chromophores [11].

A theoretical structure of α-helical poly(L-lysine) carrying P and N molecules at a center-to-center distance of 12 Å, in the deepest minimum of total interaction energy (Eq. (5)), is illustrated in Fig. 10. The interprobe edge-to-edge (carbon–carbon) distance is 6.03 Å, and the separation distance between the center of P and N groups and the helical axis is 5.94 and 6.23 Å, while the angle of the rings with respect to the helical axis is 85° and 84°, respectively. The proximity of the probes is now responsible for distortions from the ideal

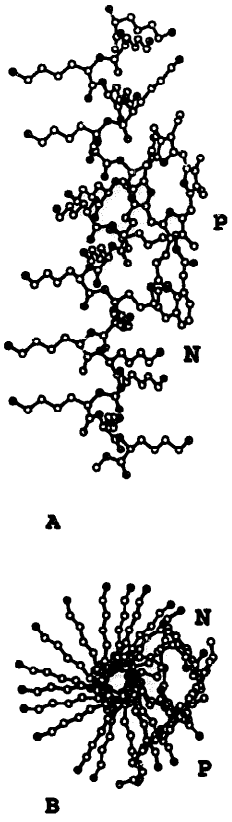

Fig. 10. (a) Molecular model of α-helical poly(L-lysine) carrying P and N chromophores at a center-to-center distance of 11.53 Å and an edge-to-edge distance of 6.03 Å, in the deepest minimum of total energy (see text). The separation distance between the center of P and N groups and the helical axis is 5.94 and 6.23 Å, respectively. For clarity, two side-chains closest to the porphyrin moiety are eliminated. (b) Same structure viewed along the helical axis. Nitrogen atoms are in black.

structures, i.e. those carrying one chromophore only (Fig. 9), because not all side-chains can be well accommodated.

Irrespective of the model used to describe the transfer process [23–25], a requirement for efficient electron transfer is that the reacting species be appropriately coupled vibronically in the transition state. The arrangement shown in Fig. 10, reminiscent of heme edge-to-heme edge geometry in interacting electron transport proteins [30,31], appears suitable for the purpose, in that the rather rigid assembly of the α-helical structure with the donor and acceptor molecules lying on its surface could maintain the proper vibrational modes of the interacting P and N* species, playing a critical role in facilitating the electron transfer process.

Where the same molecular mechanics calculations (Eq. (5)) were applied to the α-helical oligopeptides, a quite different topology results, as illustrated in Fig. 11, where the deepest minimum energy structures of the octa- and decapeptide are reported. The transfer efficiency of both conformers, calculated by Eq. (1) [13], closely agrees with that experimentally determined, Eq. (4), i.e. 0.88 vs. 0.86 for $P(Ala)_2N$ and 0.79 vs. 0.76 for $P(Ala)_4N$, leading us to consider the present theoretical models as a good representation of the actual compounds undergoing energy transfer.

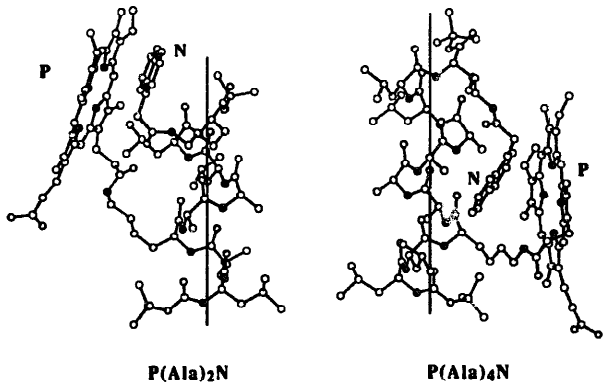

Fig. 11. Molecular model of α-helical $P(Ala)_2N$ and $P(Ala)_4N$ in the deepest energy minimum, viewed perpendicularly to the helical axis. The probes exhibit an almost face-to-face arrangement, with a center-to-center distance of 6.95 and 5.96 Å and an angle between the rings of about 19° and 39°, respectively. Nitrogen atoms are in black.

The two chromophores this time attain a stacked, almost face-to-face geometry, probably because the backbone chains are too short for allowing an edge-to-edge arrangement. The center-to-center distance is 6.95 and 5.96 Å for $P(Ala)_2N$ and $P(Ala)_4N$, and the angle between the planes of the porphyryl and naphthyl rings is about 19° and 39°, respectively. The interchromophoric separation is hence large enough to minimize orbital overlap effects [32], and the overall topology is suitable for a dipole–dipole interaction mechanism, as that of the Förster model for energy transfer [15], which was successfully applied by us to the quenching process of N* in the oligopeptides examined [12,13].

In conclusion, further experiments are clearly required for a better understanding of the observed phenomena, but the computed structures reported here ascertain that the arrangement of the probes bound to the ordered matrix and the quenching mechanism of naphthalene are closely related. The picture that emerges is, in fact, that the quite different topologies of the systems investigated are primarily responsible for the observed electron transfer/energy transfer transition.

Acknowledgements

We thank Professor R. Righini (University of Florence) and Dr. F. Elisei (University of Perugia) for helpful discussions. This work was supported in part by the National Research Council (C.N.R.) and in part by a Commission of the European Communities under contract No. Ge1*CT92-0046.

References

[1] J.D. Batteas, A. Harriman, Y. Kanda, N. Mataga and A.K. Nowak, *J. Am. Chem. Soc.*, *112* (1990) 126; S. Knapp, T.G.M. Dhar, J. Albaneze, S. Gentemann, J.A. Potenza, D. Holten and H.J. Schugar, *J. Am. Chem. Soc.*, *113* (1991) 4010; A. Helms, D. Heiler and G. McLendon, *J. Am. Chem. Soc.*, *114* (1992) 6227.

[2] M.R. Wasielewski, *Chem. Rev.*, *92* (1992) 435, and references cited therein.
[3] J.-Y. Liu, J.A. Schmidt and J.R. Bolton, *J. Phys. Chem.*, *95* (1991) 6924; M. Antolovich, P.J. Keyte, A.M. Oliver, M.N. Paddon-Row, J. Kroon, J.W. Verhoeven, S.A. Jonker and J.M. Warman, *J. Phys. Chem.*, *95* (1991) 1933.
[4] A.V. Vannikov and A.D. Grishina, *Russ. Chem. Rev., Ingl. Trasl.*, *58* (1989) 1169, and references cited therein.
[5] M. Sisido, R. Tanaka, Y. Inai and Y. Imanishi, *J. Am. Chem. Soc.*, *111* (1989) 6790; Y. Inai, M. Sisido and Y. Imanishi, *J. Am. Chem. Soc.*, *95* (1991) 3847; Y. Inai, M. Sisido and Y. Imanishi, *J. Phys. Chem.*, *94* (1990) 6237–6243, 8365–8370.
[6] B. Pispisa, A. Palleschi and M. Venanzi, *Trends Phys. Chem.*, *2* (1991) 153.
[7] S. Inoue, T. Sano, Y. Yakabe, H. Ushio and T. Yasugana, *Biopolymers*, *18* (1979) 681.
[8] B. Bednár, H. Morawetz and J.A. Shafer, *Macromolecules*, *18* (1985) 1940; D. Ying Chu and J.K. Thomas, *J. Phys. Chem.*, *89* (1985) 4065.
[9] C.A. McWherter, E. Haas, A.R. Leed and H.A. Scheraga, *Biochemistry*, *25* (1986) 1951.
[10] (a) B. Pispisa, M. Venanzi and M. D'Alagni, *Biopolymers*, *34* (1994) 435. (b) B. Pispisa, M. Venanzi and A. Palleschi, *J. Chem. Soc. Faraday Trans.*, *90* (1994) 1857.
[11] B. Pispisa, A. Palleschi, M. Venanzi and G. Zanotti, in R.S. Hodges and J.A. Smith (eds.), *Peptides: Chemistry, Structure and Biology*, ESCOM, Leiden, 1994, p. 812; B. Pispisa, M. Venanzi, A. Palleschi and G. Zanotti, *Biopolymers*, *36* (1994) 497.
[12] (a) B. Pispisa, M. Venanzi, A. Palleschi and G. Zanotti, *J. Mol. Liquids*, *61* (1994) 167. (b) B. Pispisa, M. Venanzi, A. Palleschi and G. Zanotti, *Macromolecules*, *27* (1994) 7800.
[13] B. Pispisa, A. Palleschi, M. Venanzi and G. Zanotti, *J. Phys. Chem.*, *100* (1996) 6835.
[14] P.Y. Chou and G.D. Fasman, *Ann. Rev. Biochem.*, *47* (1978) 251; S. Marqusee, V.H. Robbins and R.L. Baldwin, *Proc. Natl. Acad. Sci. USA*, *86* (1989) 5286.
[15] T. Förster, *Ann. Phys.* (Leipzig), *2* (1948) 55.
[16] I.Z. Steinberg, *J. Chem. Phys.*, *48* (1968) 2411; A. Grinvald, E. Haas and I.Z. Steinberg, *Proc. Natl. Acad. Sci. USA.*, *69* (1972) 2273.
[17] B. Valeur, J. Mugnier, J. Pouget, J. Bourson and F. Santi, *J. Phys. Chem.*, *93* (1989) 6073; M. Kaschke, N.P. Ernsting, B. Valeur and J. Bourson, *J. Phys. Chem.*, *94* (1990) 5757.
[18] R.S. Sinclair, D. Tait and T.G. Truscott, *J. Chem. Soc., Farady I*, *76* (1980) 417.
[19] P.K. Chatterjee, K. Kamioka, J.D. Batteas and S.E. Webber, *J. Phys. Chem.*, *95* (1991) 960.
[20] G.S. Nahor, J. Rabani and F. Grieser, *J. Phys. Chem.*, *85* (1981) 697.
[21] D.F. Eaton, *Pure Appl. Chem.*, *60* (1988) 1107.
[22] B. Kr. Manna, D. Sen, S. Ch. Bera and K.K. Rohatgi-Mukherjee, *Chem. Phys. Lett.*, *176* (1991) 191.
[23] R.A. Marcus and N. Sutin, *Biochim Biophys. Acta*, *811* (1985) 265; M.D. Newton, *Chem. Rev.*, *91* (1991) 767.
[24] See, for example, *Electron and Proton Transfer*, *J. Chem. Soc., Faraday Discuss.*, *74* (1982).
[25] J.W. Evenson and M. Karplus, *Science*, *26* (1993) 1247, and references cited therein.
[26] P.J. Flory, *Statistical Mechanics of Chain Molecules*, Intescience, New York, 1969; W.L. Mattice and U.W. Suter, *Conformational Theory of Large Molecules*, Wiley, New York, 1994.
[27] M.C. Manning, M. Illangasekare and R.W. Woody, *Biophys. Chem.*, *31* (1988) 77.
[28] N.L. Allinger, *J. Am. Chem. Soc.*, *99* (1977) 8127; U. Burkert and N.L. Allinger, *Molecular Mechanics*, American Chemical Society, Washington, DC, 1982.
[29] (a) B. Pispisa, A. Palleschi, M. Barteri and S. Nardini, *J. Phys. Chem.*, *89* (1985) 1767. B. Pispisa and A. Palleschi, *Macromolecules*, *19* (1986) 904. (b) B. Pispisa, A. Palleschi and G. Paradossi, *J. Phys. Chem.*, *91* (1987) 1546; B. Pispisa, G. Paradossi, A. Palleschi and A. Desideri, *J. Phys. Chem.*, *92* (1988) 3422; E. Chiessi, A. Palleschi, G. Paradossi, M. Venanzi and B Pispisa, *J. Chem. Res. (S)* (1991) 248; E. Chiessi, M. Branca, A. Palleschi and B. Pispisa, *Inorg. Chem.*, *34* (1995) 2600.
[30] F.R. Salemme, in B. Chance, D.C. DeVault, H. Frauenfelder, R.A. Marcus, J.R. Schrieffer and N. Sutin (eds.), *Tunneling in Biological Systems*, Academic Press, New York, 1979, p.523.
[31] D.W. Dixon, X. Hong, S.E. Woehler, A.G. Mauk and B.P. Sishta, *J. Am. Chem. Soc.*, *112* (1990) 1082.
[32] G.D. Scholes and K.P. Ghiggino, *J. Phys. Chem.*, *98* (1994) 4580.